AD-A095 308 FOREIGN TECHNOLOGY DIV WRIGHT-PATTERSON AFB OH F/G 20/2
STUDY OF THE GROWTH OF VACUUM CONDENSED AU PARTICLES ONTO THE (--ETC(U)
JAN 81 M I BIRJEGA, V TOPA, V TEODORESCU

UNCLASSIFIED FTD-ID(RS)T-1685-80 NL

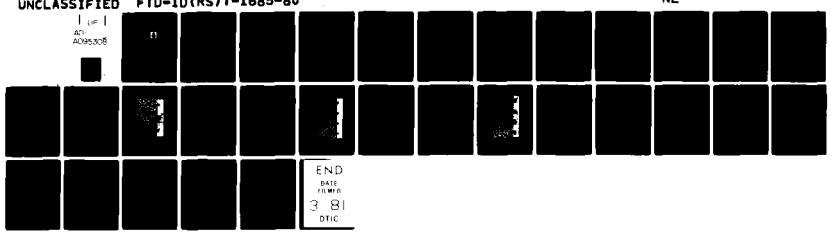

FTD-ID(RS)T-1685-80

(2)

FOREIGN TECHNOLOGY DIVISION

STUDY OF THE GROWTH OF VACUUM CONDENSED Au PARTICLES ONTO THE (100) SURFACES OF KBr, KCl AND NaCl SUBSTRATES WITH COLLOIDAL CENTRES

by

M. I. Birjega, V. Topa and V. Teodorescu

EDITED TRANSLATION

FTD-ID(RS)T-1685-80 7 January 1981

MICROFICHE NR: FTD-80-C-001250

STUDY OF THE GROWTH OF VACUUM CONDENSED Au PARTICLES ONTO THE (100) SURFACES OF KBr, KCl AND NaCl SUBSTRATES WITH COLLOIDAL CENTRES

By: M. I. Birjega, V. Topa and V. Teodorescu

English pages: 28

Source: Studii si Cercetari de Fizica, Vol. 30, Nr. 2, 1978, pp. 179-188 plus 4 unnumbered pages, 189-190

Country of origin: Romania
Translated by: SCITRAN
F33657-78-D-0619
Requester: FTD/TQTD
Approved for public release; distribution unlimited

PREPARED BY:

TRANSLATION DIVISION
FOREIGN TECHNOLOGY DIVISION
WP-AFB, OHIO.

(14) FTD-ID-(RS)T-1625-77

(11) 7 Jan 82

(6) STUDY OF THE GROWTH OF VACUUM CONDENSED AU PARTICLES ONTO THE (100) SURFACES OF KBr KCl AND NaCl SUBSTRATES WITH COLLOIDAL CENTRES

(Studiul formarii agregatelor de Au condensate in vid pe suprafata (100) a substratelor de KBr, KCl and NaCl cu centrii coloidali),

(10) M. I. Birjega, V. Topa and V. Teodorescu

St. Cerc. Fiz., Vol. 30(2),
pp. 179-196, 1978

1. Introduction

A series of deposits of Au with thinness equivalent t, of 4.5, 6.0, 9.0 and 12 Å was carried out under high vacuum conditions at substrate temperatures of 290, 260 and 170°C and at a deposit rate of 0.3 and 0.1 Å $\cdot$ s^{-1} on the surface (100) of crystals of KBr ($7.7 \cdot 10^{9}$ cm^{-2} Cu colloids), KCl ($8.4 \cdot 10^{10}$ cm^{-2} Pb colloids), NaCl ($1.2 \cdot 10^{10}$ cm^{-2} Cu colloids), NaCl ($5.2 \cdot 10^{8}$ cm^{-2} Cu colloids) and NaCl ($3.6 \cdot 10^{10}$ cm^{-2} Ag colloids). Electron microscope images of the deposits made it possible to determine, as a function of size, their equivalent t, the specific density n_x of the aggregates, the proportion of S_{100} and S_{111} oriented aggregates, the degree of surface coverage with Å aggregates, and the mean diameter $\bar{D}$ of the aggregate distribution.

Histograms of the aggregate distribution on a standard area A were plotted for all of the deposits made for the purpose of producing evidence on the processes of growth, coalescence and secondary nucleation of the Au aggregates as a function of diameter interval.

2. Experimental Methodology and Data Calculation

2.1. Experimental Conditions for Achieving Au Deposits

Deposits of Au with equivalent thicknesses of 4.5, 6.0, 9.0 and 12 Å were made simultaneously in a high vacuum ($2 \cdot 10^{-6}$ mm Hg) on (100) surfaces of KBr, KCl and NaCl, cleaved in air and heated to 290, 260 or 170°C. Contamination of the alkali halide surfaces because of cleavage in the environmental atmosphere was improved to a great degree by applying the desorption process of Rossow, Kotze and Henning [1]. Regardless of the temperature at which the Au deposition was made, the substrates were maintained for an hour in a vacuum of $2 \cdot 10^{-6}$ mm Hg at a temperature of 300°C.

Crystals of KBr, KCl and NaCl, grown by Kyropoulos' method, were treated and dyed electrolytically in order to obtain Cu, Pb or Ag colloids [2].

Au aggregates were formed with continuous flux (C) at a deposition rate of 0.3 Å $\cdot$ s^{-1} or 0.1 Å $\cdot$ s^{-1}.

In order to preserve their crystallographic shape and orientation, the Au aggregates were covered with a thin carbon layer approximately 200 Å thick. The Au particles covered with the carbon layer were precipitated on the alkali halide substrates by immersion in water distilled twice and collected on a special copper grid. The study of the specimens prepared in this way was conducted with a JEM-120 microscope.

2.2. Methodology of Determining the Characteristic Magnitudes of the Nucleation Process

Electron microscope images, made at a magnification of 100,000, in a zone without any coloration effects, constituted the source of data necessary to determine the characteristic magnitudes of the processes of formation and growth of Au aggregates. The Au aggregates were counted by photographing the electron microscope images, enlarged 4 times over the original magnification (x 400,000) as a function of

-- their dimensions by diameter intervals (up to 25 Å, 25 to 50 Å, 50 to 75 Å and so on);

-- their morphology (square, triangular and of other shapes).

The aggregates were counted according to total area A, at 2 $\cdot$ 10^7 $Å^2$. In studying the nucleation kinetics of Au on a NaCl substrate, Donohoe and Robins [3] considered aggregates formed on areas from 1.12 $\cdot$ 10^7 $Å^2$ to 2.24 $\cdot$ 10^7 $Å^2$, while Schmeisser [4] considered an area of 1.4 $\cdot$ 10^7 $Å^2$. In order to make a quantitative estimate of the uniformity of the nucleation process [5], the total area was divided into 20 squares of 1,000 Å on each

side. This formed the elementary surface on which the aggregates were counted as a function of size and shape. Table 1 presents the way in which the data mentioned were taken from electron microscope images in the case of some Au particles on a KCl substrate with Pb colloids.

Microscopic and electron diffraction research on the Au aggregates formed by vacuum deposition on (100) cleavage surfaces of some ionic crystals conducted in a series of laboratory tests [6-12] demonstrated the existence of the following types of aggregates:

-- aggregates square or rectangular in orientation (100);

-- aggregates triangular in orientation (111);

-- multiple twin-crystal aggregates or multiple twin-crystal particles (PMM), pentagonal, hexagonal or rhomboid with specific contrast effects. The types mentioned should be further increased by a series of aggregates which do not exhibit any definite geometric shape. This category includes very small aggregates which had not reached a phase of equilibrium and very large aggregates due to coalescence processes.

2.2.1. Specific Density n_x of the Aggregates

The specific density n_x of the aggregates was obtained as a result of counting the aggregates visible in all 20 elementary areas, and applying the equation

$$n_x = \frac{\sum_{k=1}^{20} n_k}{20} \cdot 10^{10}\text{cm}^{-2}. \quad (1)$$

The standard deviation in all 20 series of measurements was obtained from the equation

$$S = \sqrt{\frac{\sum_{k=1}^{20} (n_k - n_x)^2}{19}} \cdot 10^{10}\text{cm}^{-2}. \quad (2)$$

Table 1

1 Total agregate				2 Numărul agregatelor în funcție de diametru în Å și de forma :											
				3 până la 25			4 25 la 50			5 50 la 75			6 75 la 100		
	n_Σ	n_Σ^{100}	n_Σ^{111}	7 pătrat	8 triunghi	9 alte forme	7 pătrat	8 triunghi	9 alte forme	7 pătrat	8 triunghi	9 alte forme	7 pătrat	8 triunghi	9 alte forme
1	32	13	1	–	–	10	3	–	2	9	1	6	1	–	–
2	40	18	–	–	–	8	3	–	4	15	–	10	–	–	–
3	33	13	–	–	–	5	3	–	4	10	–	11	–	–	–
4	25	9	1	–	–	2	3	–	3	6	1	10	–	–	–
5	42	15	1	–	–	6	4	–	8	11	1	12	–	–	–
6	41	12	–	–	–	8	5	–	7	9	–	14	–	–	–
7	43	15	–	–	–	6	4	–	8	10	–	14	1	–	–
8	36	14	1	–	–	5	5	–	6	8	1	9	1	–	1
9	40	14	1	–	–	11	4	–	4	10	1	10	–	–	–
10	48	15	1	–	–	13	5	–	7	10	1	11	–	–	1
11	38	12	–	–	–	7	3	–	7	9	–	12	–	–	–
12	46	14	–	–	–	11	3	–	8	9	–	13	2	–	–
13	37	14	3	–	–	7	5	–	6	9	3	7	–	–	–
14	48	14	3	–	–	9	6	–	12	8	2	10	–	–	–
15	44	12	1	–	–	6	2	–	7	10	1	18	–	–	–
16	35	14	–	–	–	7	1	–	3	12	–	10	1	–	1
17	42	13	–	–	–	8	3	–	7	10	–	11	–	–	–
18	38	14	2	–	–	7	4	–	8	10	2	7	–	–	–
19	36	13	–	–	–	6	2	–	5	11	–	12	–	–	–
20	41	13	2	–	–	11	3	–	6	10	2	9	–	–	–
Σ	781	271	17	–	–	153	69	–	122	196	17	219	6	–	3

Key: 1-Total aggregates, 2-Number of aggregates as a function of diameter in A and of shape, 3-Up to 25, 4-25 to 50, 5-50 to 75, 6-75 to 100, 7-Square, 8-Triangle, 9-Other shapes

2.2.2. Degrees of Orientation S_{100} and S_{111}

The degree of epitaxial orientation S_{100} was determined from the equation

$$S_{100} = \frac{\sum_{k=1}^{20} n_k^{100}}{\sum_{k=1}^{20} n_k} \cdot 100\%, \tag{3}$$

in which $\sum_{k=1}^{20} n_k$ represents the total number of aggregates enumerated in the entire 20 elementary areas, while $\sum_{k=1}^{20} n_k^{100}$ is the total number of aggregates whose shape is square (Table 1). The degree of orientation S_{111} was obtained by applying a similar equation

$$S_{111} = \frac{\sum_{k=1}^{20} n_k^{111}}{\sum_{k=1}^{20} n_k} \cdot 100\%, \tag{4}$$

in which $\sum_{k=1}^{20} n_k^{111}$ represents the total number of aggregates for the standard A_s area, whose shape is triangular. Images of electron diffraction obtained from the respective areas were used to verify the values determined for S_{100} and S_{111} from the electron microscope images in conformity with equations (3) and (4). Thus the method adopted by us to evaluate the degree of orientation unites the two methods used in the specialized literature by Harsdorff [13] and Ino et al. [14].

2.2.3. Histogram of Distribution of Aggregates as a Function of Their Diameter

The histogram of distribution of the aggregates as a function of their diameter was plotted on the basis of data recorded in tables, similar to Table 1. The histograms, standardized for all particles in standard area A_s, exhibit the density distribution of aggregates by diameter intervals from 25 to 25 Å. [sic]. The hatched sections of the histograms represent the number corresponding to the aggregates of square shape in epitaxial orientation (100).

2.2.4. The Degree of Z Coverage of the Substrate with Aggregates

Making an approximate consideration that all of the aggregates have the shape of a spherical cap [15], the degree of Z (%) coverage of the surface with aggregates was determined from the equation

$$Z = \frac{\sum_{i=1,2,3,\ldots} n_i a_i}{A_s} 100\% \qquad (5)$$

in which n_i represents the number of aggregates in a diameter interval on a histogram, while a_i is the area of aggregates corresponding to the maximum diameter of the interval.

2.2.5. Mean Diameter $\bar{D}$ of the Aggregates

In a corresponding way the mean diameter of the aggregates was obtained from the equation

$$\bar{D} = 2 \sqrt{\frac{\sum_{i=1,2,3,\ldots} n_i a_i}{\pi \sum_{k=1}^{20} n_k}} \qquad (6)$$

3. Experimental Results

A compilation of the experimental data obtained by processing electron microscope images and electron diffraction of the Au aggregates on alkali halide substrates with colloidal centers is contained in Tables 2 and 3. The tables indicate the substrates with their content and type of defects, equivalent thickness of particles (t), formation period of aggregates, deposition conditions (substrate temperature T, deposition rate R) and values obtained for the parameters which characterize the process of Au aggregate formation (n_x, Z, $\bar{D}$, S_{100} and S_{111}). Figures 1, 4 and 7 graphically represent the dependence of the magnitudes n_x, Z, $\bar{D}$ and S_{100} for the KBr, KCl and NaCl substrates with respect to equivalent thickness t of particles and deposition conditions (T and R). The histograms in Figures 2, 5 and 8 present the

Table 2

	1 Grosimea echivalentă a depunerii Å	2 Durata formării agregatelor s	3 Condiții de depunere T °C	R Å · s⁻¹	Flux	4 Valori obținute pentru parametri $n_r = S$ 10^{10} cm⁻²	Z %	D Å	S_{100} %	S_{111}
5 Substratul: KBr ($7{,}7 \cdot 10^{1}$ · cm⁻² 6 coloizi Cu)										
1	4,5	15	290	0,3	C	21 ± 3	20	111	57	
2	12,0	40	290	0,3	C	13 ± 1	30	169	61	
3	6,0	60	290	0,1	C	16 ± 2	23	126	72	1
4	9,0	90	290	0,1	C	39 ± 3	21	80	65	1
5	6,0	20	260	0,3	C	19 ± 2	9	78	61	
6	12,0	40	260	0,3	C	15 ± 2	11	96	60	
7	4,5	15	170	0,3	C	27 ± 4	29	114	23	
5 Substratul: KCl ($8{,}4 \cdot 10^{10}$ · cm⁻² 7 coloizi Pb)										
1	4,5	15	290	0,3	C	34 ± 4	14	72	25	1
2	6,0	20	290	0,3	C	38 ± 4	16	74	41	–
3	9,0	30	290	0,3	C	30 ± 3	24	102	41	3
4	12,0	40	290	0,3	C	25 ± 3	28	118	37	2
5	6,0	60	290	0,1	C	26 ± 3	15	86	33	–
6	9,0	90	290	0,1	C	44 ± 4	23	81	36	1
7	6,0	20	260	0,3	C	25 ± 4	5	52	–	–
8	12,0	40	260	0,3	C	35 ± 4	11	62	23	–

Key: 1-Equivalent thickness of deposits Å, 2-Period of aggregate formation s, 3-Deposit conditions, 4-Values obtained for parameters, 5-Substrate, 6-Cu colloids, 7-PB colloids

Table 3

	1 Grosimea echivalentă a depunerii Å	2 Durata formării agregatelor s	3 Condiții de depunere T °C	R Å · s⁻¹	Flux	4 Valori obținute pentru parametri $n_s = S$ 10^{10} cm^{-2}	Z %	$\bar{D}$ Å	S_{100} %	S_{111} %
5 Substratul: NaCl($1{,}2 \cdot 10^{10}$ cm^{-2} 6 coloizi Cu)										
1	4,5	15	290	0,3	C	20 ± 3	10	77	–	–
2	6,0	20	290	0,3	C	35 ± 4	10	57	–	–
3	9,0	30	290	0,3	C	25 ± 3	17	94	3	3
4	12,0	40	290	0,3	C	32 ± 2	44	136	6	14
5	9,0	90	290	0,1	C	46 ± 6	21	76	13	6
6	12,0	40	260	0,3	C	17 ± 4	8	79	3	1
5 Substratul: NaCl($5{,}2 \cdot 10^{9}$ cm^{-2} 6 coloizi Cu)										
1	4,5	15	290	0,3	C	21 ± 2	12	82	–	–
2	6,0	20	290	0,3	C	27 ± 3	10	68	2	–
3	9,0	30	290	0,3	C	28 ± 4	24	105	4	5
4	12,0	40	290	0,3	C	27 ± 3	33	124	5	6
5	9,0	90	290	0,1	C	55 ± 6	22	84	11	12
5 Substratul: NaCl($3{,}6 \cdot 10^{10}$ cm^{-2} 7 coloizi Ag)										
1	12,0	40	290	0,3	C	26 ± 3	47	149	8	4
2	6,0	60	290	0,1	C	21 ± 4	13	89	3,5	1
3	9,0	90	290	0,1	C	40 ± 3	20	79	23	8

Key: 1-Equivalent thickness of deposits Å, 2-Period of aggregate formation s, 3-Deposit conditions, 4-Values obtained for parameters, 5-Substrate, 6-Cu colloids, 7-Ag colloids

distribution of the Au aggregate diameters as a function of their size in the 3 alkali halide substrates formed under different deposition conditions and aggregate growth phases.

The electron microscope images and the electron diffraction in Figures 3, 6 and 9 illustrate the different aspects associated with the morphology and kinetics of Au aggregate growth.

3.3. KBr Substrate ($7.7 \cdot 10^{9}$ cm^{-2} Cu Colloids)

The results obtained for Au deposition on the KBr substrate with Cu colloids are presented in Table 2 and Figures 1, 2 and 3. The aggregates formed at 290 and 260°C at a deposition rate of 0.3 $\mathring{A} \cdot s^{-1}$ reveal a drop in their n_x value in the value interval corresponding to some equivalent thicknesses from 4.5 to 12 $\mathring{A}$ (Figure 1). This can be explained by the fact that under these deposition conditions the maximum saturation density of N_s aggregates, occurring at equivalent thicknesses smaller than 4.5 $\mathring{A}$, and the later reduction in aggregate density at the same time as the growth of the equivalent thickness of the particles can be attributed only to the colascence processes (Figures 2 and 3). The percentage of aggregates of epitaxial orientation S_{100} reaches the value of approximately 60% of the aggregates formed at substrate temperature of 290 and 260°C with a deposition rate of 0.3 $\mathring{A} \cdot s^{-1}$, and remains practically constant within the interval of equivalent thickness from 4.5 to 12 A (Table 2 and Figure 1). For Au aggregates formed at the temperature of 300°C with continuous flux from $13.8 \cdot 10^{13}$ atoms $\cdot cm^{-2} \cdot s^{-1}$ on a KBr substrate cleaved in an extremely high vacuum Puskeppel and Harsdorff [16] obtained a 60% degree of epitaxial orientation S_{100}. Despite this, for deposition made at substrate temperature of 290 and 260°C at a deposition rate of 0.3 $\mathring{A} \cdot s^{-1}$, the parameters n_x and S_{100} have approximately the same value in the interval

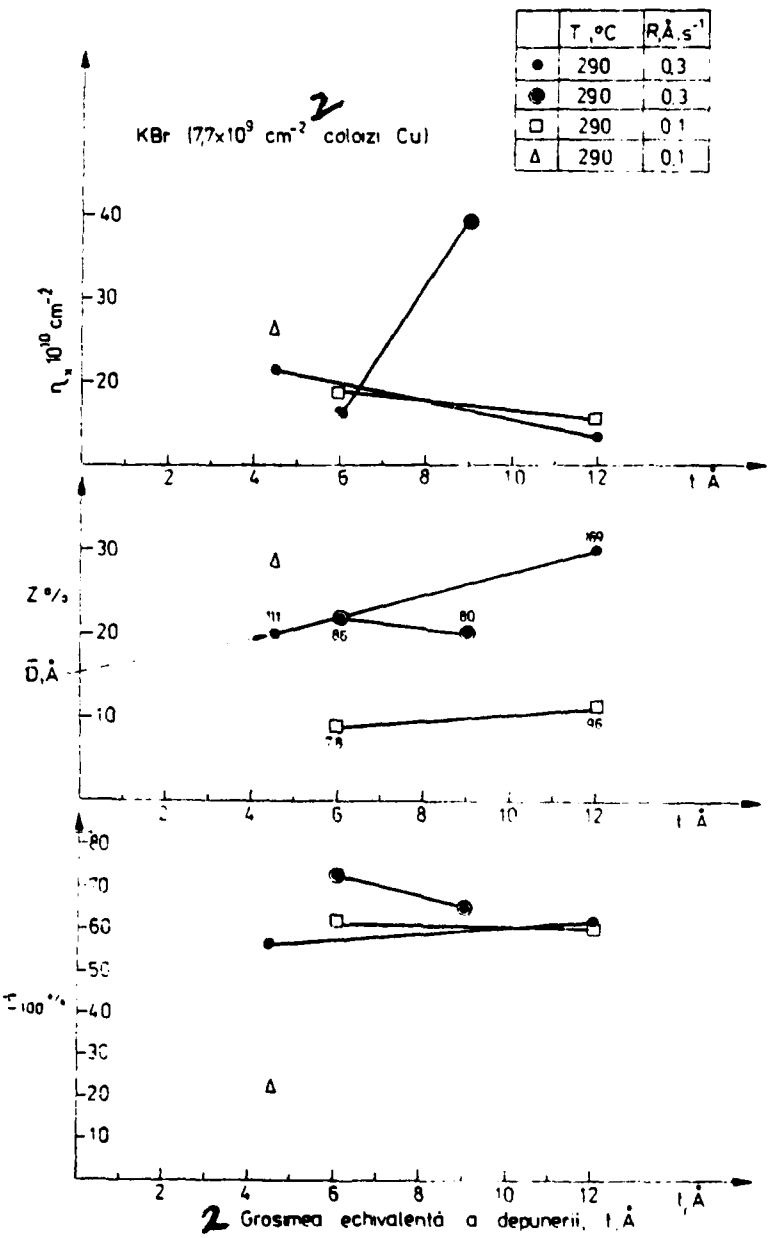

Figure 1

Dependence of parameters n_x, Z, $\bar{D}$, S_{100} and S_{111} compared by equivalent thickness t of the deposits and the deposition conditions (T and R) of aggregates of Au formed on a KBr substrate with Cu colloids.

Key: 1-Cu colloids, 2-Equivalent thickness of deposits t, Å

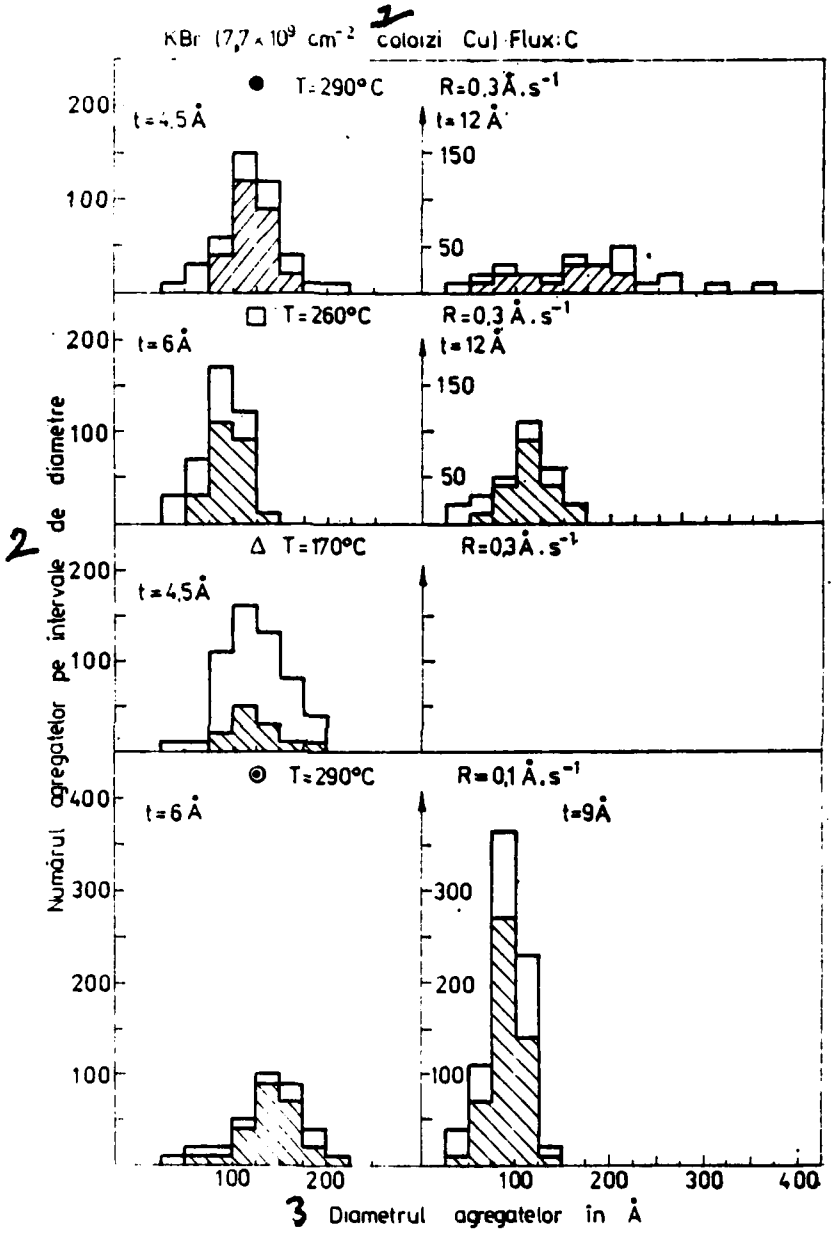

Figure 2

Histogram of distribution of diameters of Au aggregates formed under different deposition conditions (T and R) and with different equivalent thickness t on KBr substrate with Cu colloids.

Key: 1-Cu colloids, 2-Number of aggregates per diameter interval, 3-Diameter of aggregates in Å

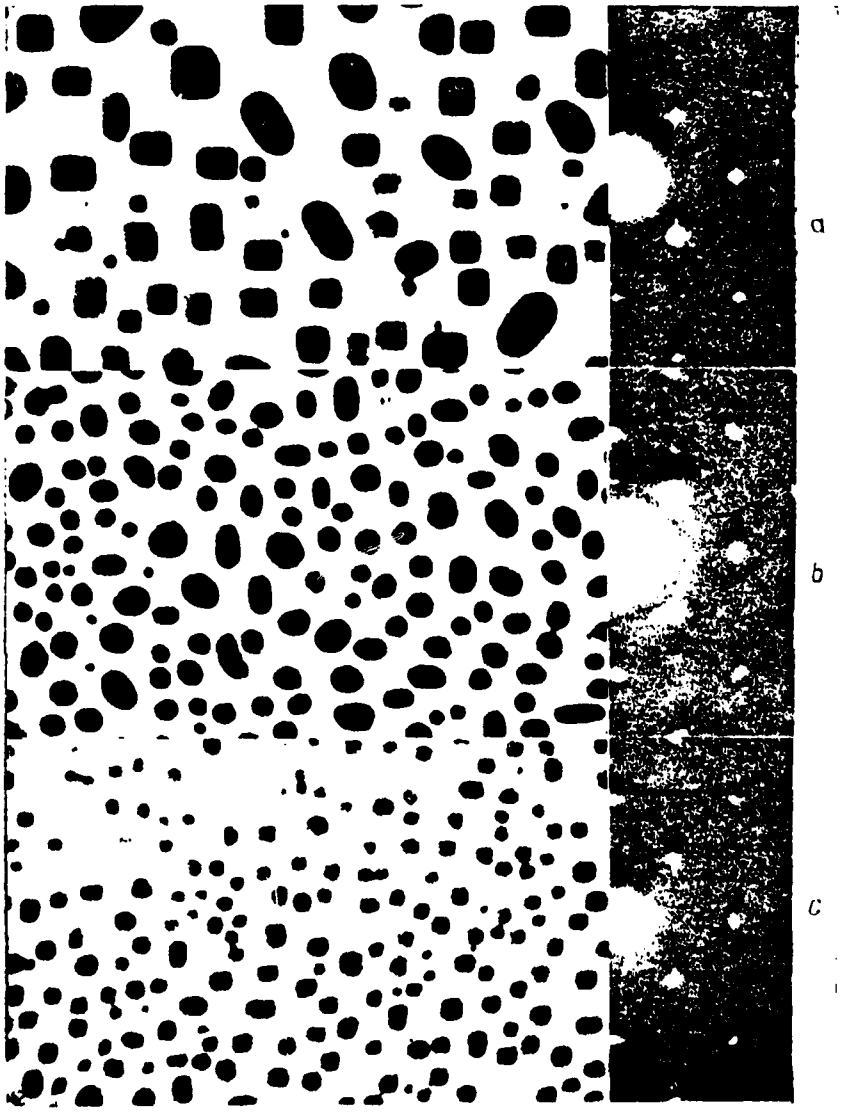

Figure 3

Microscope image (x 100,000) and diffraction of electrons of Au aggregates formed by deposition in a continuous flux on KBr substrate ($7.7 \cdot 10^9$ cm^{-2} Cu colloids)

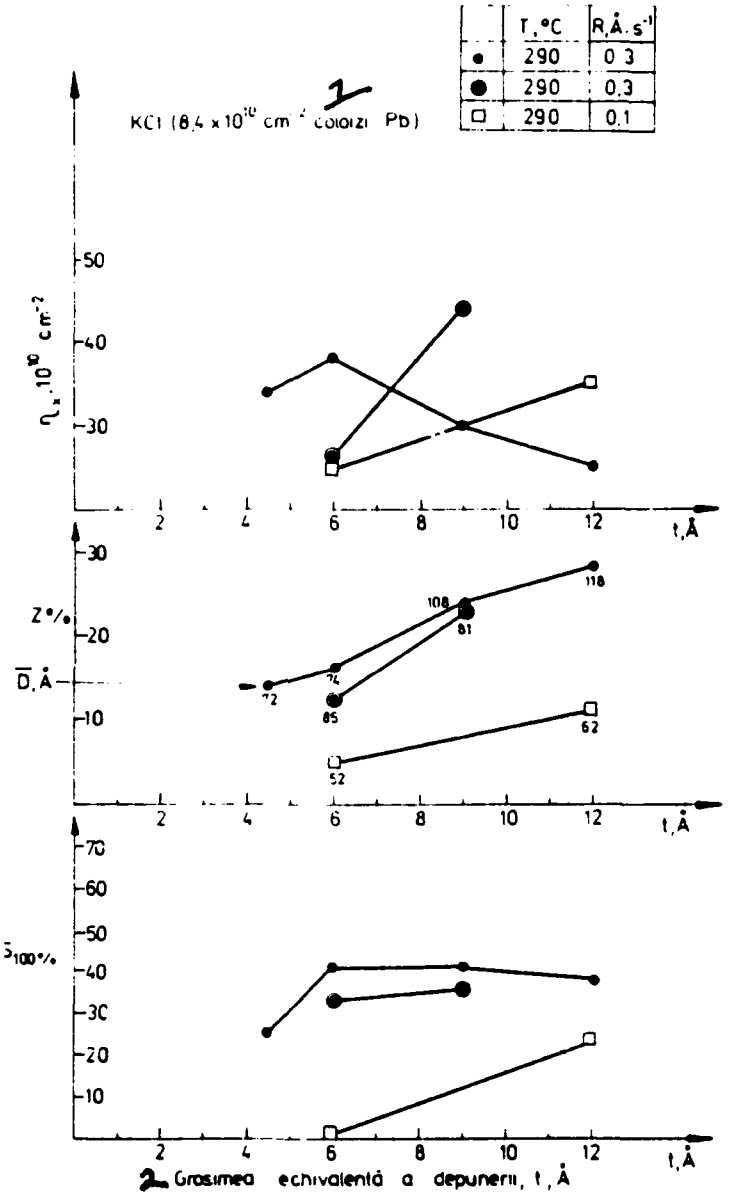

Figure 4

Dependence of parameters n_x, Z, $\bar{D}$, S_{100} and S_{111} compared by equivalent thickness t of deposits and deposition conditions (T and R) of the Au aggregates formed on a KCl substrate with Pb colloids. Key: 1-Pb colloids, 2-equivalent thickness of particles,.t, Å.

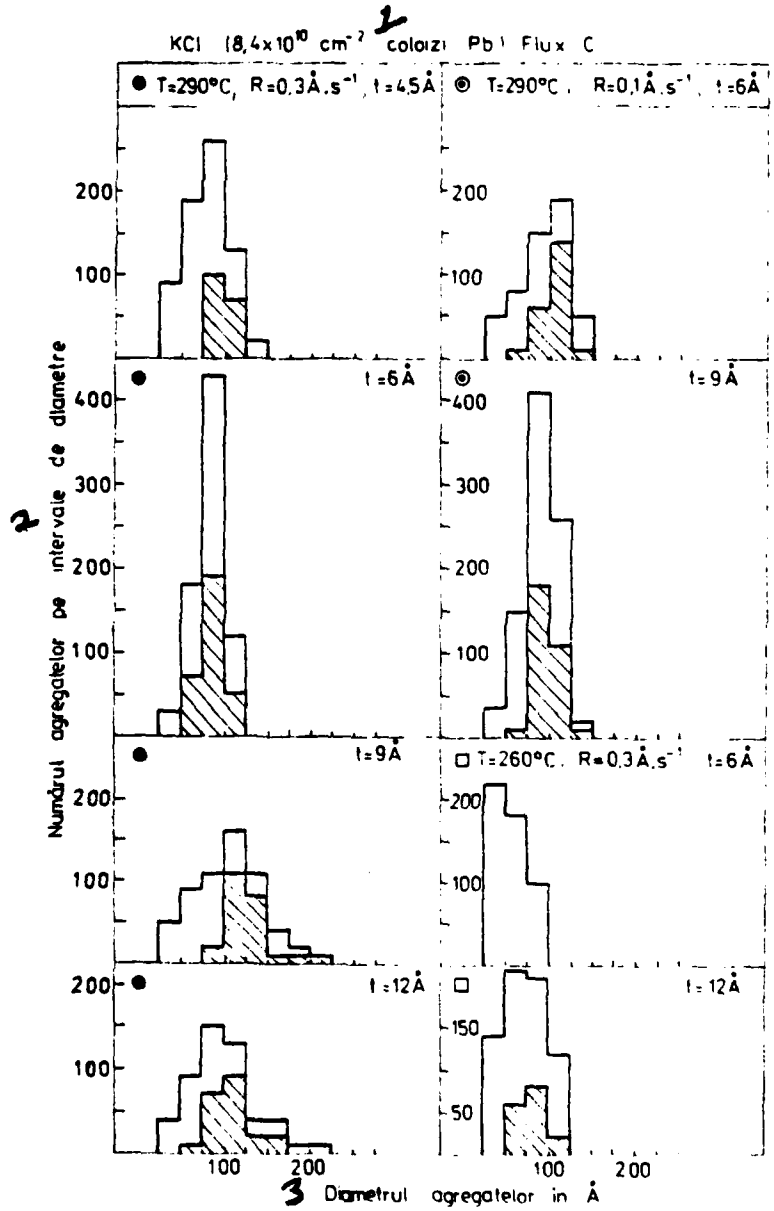

Figure 5

Histogram of distribution of diameters of Au aggregates formed under different deposition conditions (T and R) and with different equivalent thickness t on a KCl substrate with Pb colloids. Key: 1-Pb colloids, 2-diameter of aggregates in A. 3-Diameter of aggregates in Å

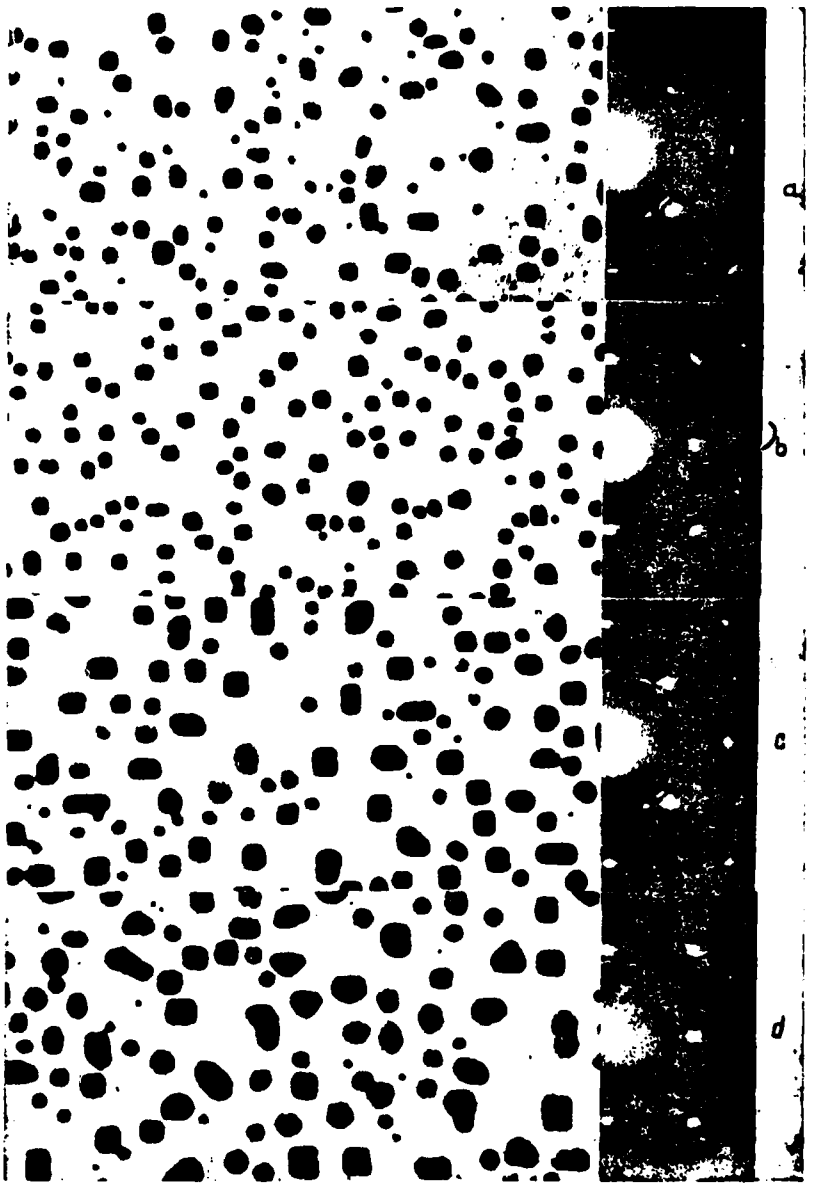

Figure 6

Microscope image (x 200,000) and diffraction of electrons of Au aggregates formed by deposition in a continuous flux on a KCl substrate ($8.4 \cdot 10^{10}$ cm^{-2} Pb colloids) at temperature T 290°C, and with deposition rate of

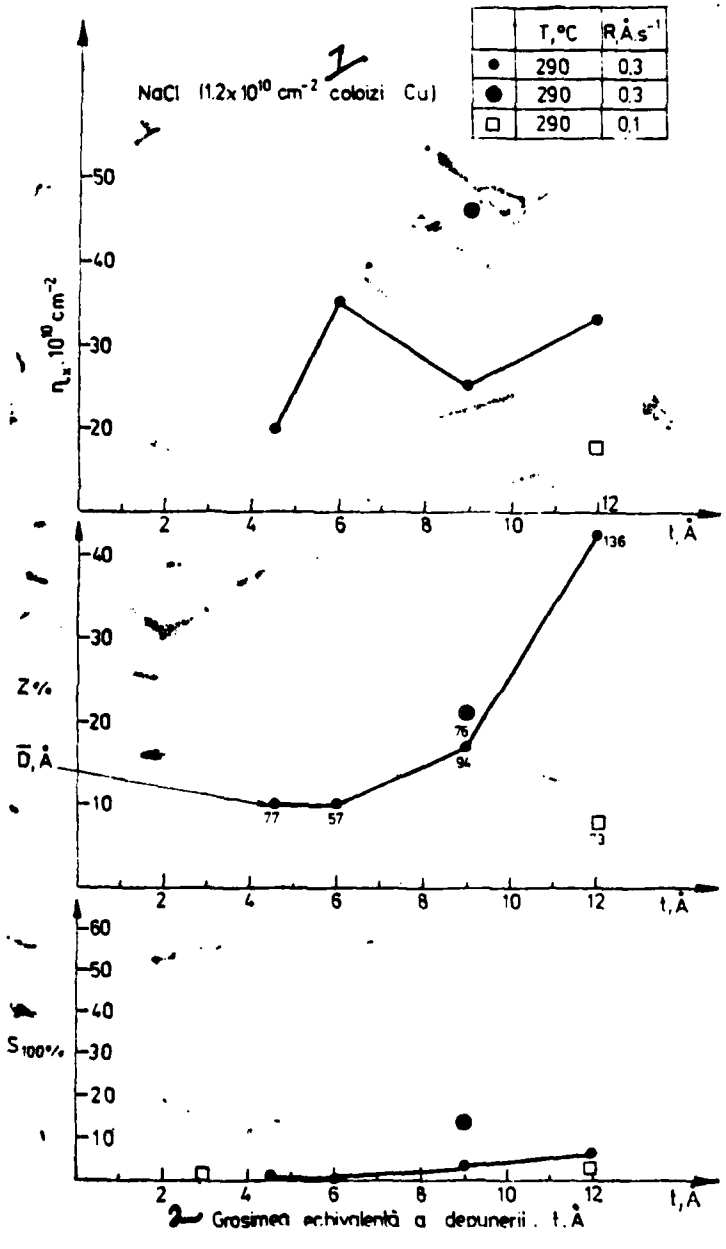

Figure 7

Dependence of parameters n_x, Z, $\bar{D}$, S_{100} and S_{111} compared for equivalent thickness t of deposits and deposition conditions (T and R) of Au aggregates formed on a NaCl substrate with Cu colloids.

Key: 1-Cu colloids, 2-Equivalent thickness of deposits, t, Å

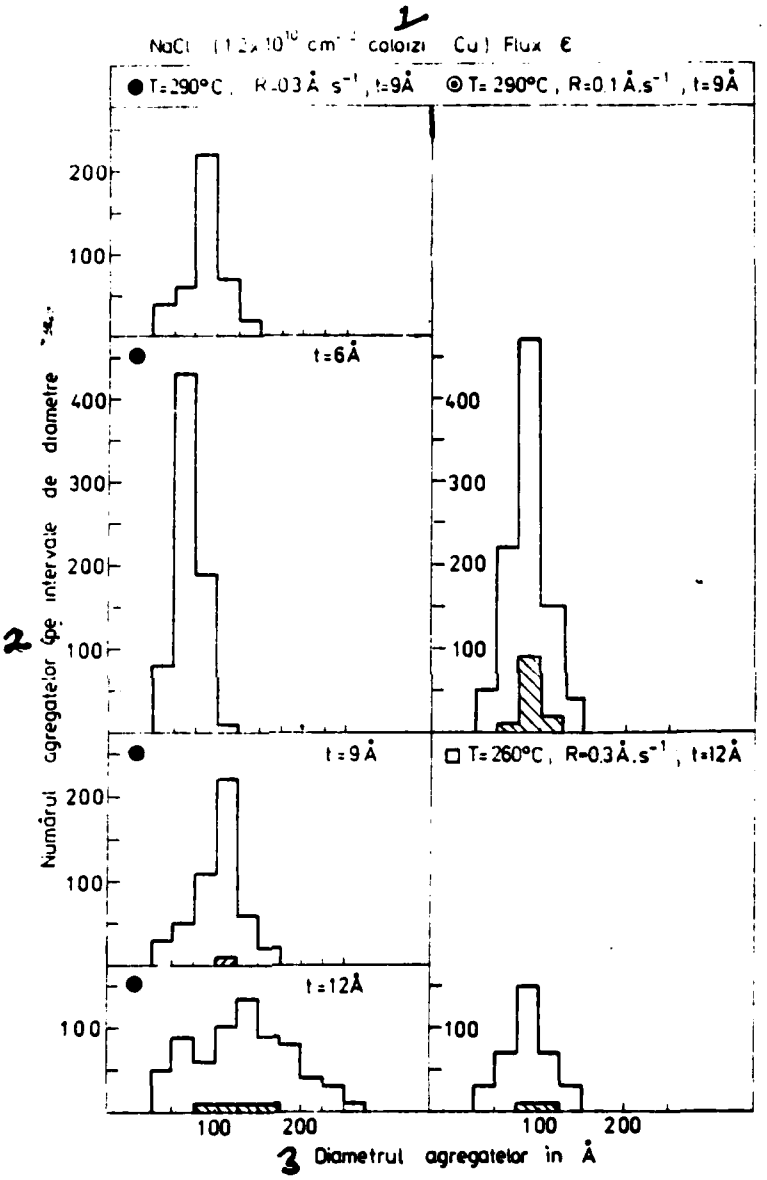

Figure 8

Histogram of distribution of diameters of Au aggregates formed under different deposition conditions (T and R) and with different equivalent thickness t on a NaCl substrate with Cu colloids.

Key: 1-Cu colloids, 2-Number of aggregates per diameter interval, 3-Diameter of aggregates in Å

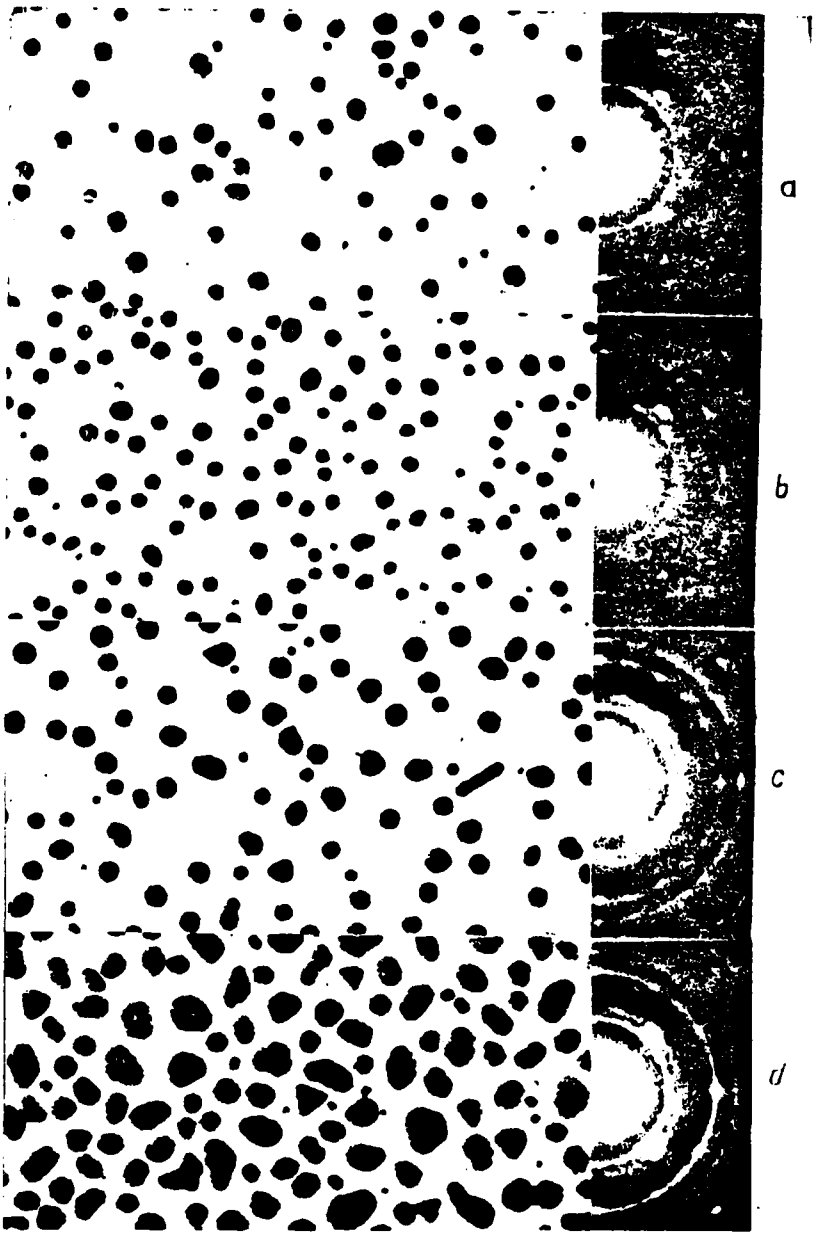

Figure 9

Microscope image (x 100,000) and diffraction of electrons of Au aggregates formed by deposition in continuous flux on a NaCl substrate ($1.2 \cdot 10^{10}$ cm^{-2} Cu colloids) at temperature t 290°C and deposition rate of

of equivalent thickness from 4.5 to 12 Å, values corresponding to the degree of Z coverage of the surface with aggregates, to the mean diameter $\bar{D}$ and varied frequency in the coalescence processes (Table 2, Figures 1, 2 and 3). The Au aggregates with equivalent thickness of 4.5 Å, formed at the substrate temperature of 290°C, have a Z coverage degree of 20% and a mean diameter of 111 Å, while aggregates formed at a substrate temperature of 260°C, while they have an equivalent thickness of 6 Å, have a 9% coverage degree and a mean diameter of 78 Å.

The histogram (Figure 2) indicates to us a greater density of Au aggregates in orientation (100) with diameters in the interval from 50 to 100 Å on deposition with an equivalent thickness of 6 Å, formed at a substrate temperature of 260°C, compared to those of 4.5 Å formed at a substrate temperature of 290°C. On the other hand, deposition with an equivalent thickness of 4.5 Å, formed at 290°C, have a greater aggregate density in orientation (100) with diameters in the intervals from 100 to 175 Å. Very intense coalescence of the aggregates with an equivalent thickness of 12 A, formed at a substrate temperature of 290°C and deposition rate of 0.3 Å $\cdot$ s^{-1}, appearing to be secondary nucleation, does not modify degree of epitaxial orientation S_{100} (Figure 2 and Figure 3a). Under these deposition conditions a degree of coverage of the surface with aggregates Z of 30% and a mean diameter of $\bar{D}$ of the aggregates of 169 Å are obtained (Figure 1), but the distribution of the diameter values of the aggregates is very great (Figure 2). The 12 Å deposition made at a substrate temperature of 260°C leads to growth of the mean diameter $\bar{D}$ of the aggregates to a value of 96 Å, instead of 78 Å, and the degree of coverage of the surface with aggregates Z of 11% instead of 9%, which takes place in growth of the equivalent deposit thickness from 6 Å to 12 Å (Table 2 and Figure 1) which is due in large degree to the growth

in the size of the aggregates because of the diffusion process of the donor atoms. As the histogram in Figure 2 indicates to us, the number of coalescent actions is very reduced. It should also be mentioned that, under these growth conditions, the percentage S_{100} of aggregates in the orientation (100) remains practically constant.

The Au aggregates, formed at a substrate temperature of 170°C, corresponding to an equivalent thickness of 4.5 Å, exhibit greater values for the specific density n_x, the degree of coverage Z and the mean diameter $\bar{D}$ in comparison with the aggregates formed at the substrate temperatures of 260 and 290°C, and the same deposition rate of 0.3 $\dot{A} \cdot s^{-1}$ (Table 2 and Figure 1). The percentage of aggregates in orientation (100) S_{100} of 20% is thus much smaller than that of the aggregates formed at higher temperatures. The reduced number of Au aggregates in orientation (100) cannot be attributed to the absence of coalescence activity, since both the histogram (Figure 2) and the electron microscope images attest to its existence (Figure 3b).

The specific density n_x of the aggregates formed at a substrate temperature of 290°C with a deposition rate of 0.1 $\dot{A} \cdot s^{-1}$ has a much greater value than that of all the above-mentioned depositions (Figure 1). The mean diameter $\bar{D}$ of the Au aggregates and the degree of coverage of the surface Z with aggregates is smaller than that of the particles made at a substrate temperature of 290°C at a deposition rate of 0.3 $\dot{A} \cdot s^{-1}$ (Figure 1 and Figure 3c). Under these deposition conditions the Au aggregates in orientation (100) reach a higher percentage, 70% compared to approximately 60% for deposition made at a deposition rate of 0.3 $\dot{A} \cdot s^{-1}$ (Figure 1). Since the number of coalescent actions is reduced at this deposition, according to what can be judged from the histogram in Figure 2, the gradual increase in epitaxial orientation S_{100} is attributed to the greater time accorded the formation of Au aggregates (Table 2) following the reduction in deposition rate.

With respect to the Au aggregates formed in an ultrahigh vacuum on a KBr substrate cleaved in situ, Puskeppel and Harsdorff [16] mention the increase in the degree of epitaxial orientation with: the increase in evaporation time, the increase in substrate temperature from 210 to 300°C, and the decrease in the deposition rate. In the initial stage of nucleation histograms of the diameter distribution of Au aggregates [16] indicate the presence of aggregates of epitaxial orientation in the domain of diameters of greater value; in the coalescence phase every large crystallite is oriented epitaxially.

3.2. KCl Substrate ($8.1 \cdot 10^{10}$ cm^{-2} Pb Colloids)

The results obtained for Au particles formed on a KCl substrate with Pb colloids are presented in Table 2 and Figures 4, 5 and 6. The specific density n_x of aggregates formed at a substrate temperature of 290°C and a deposition rate of 0.3 Å $\cdot$ s^{-1} increases in the interval of equivalent thicknesses from 4.5 to 6 Å. After reaching the maximum saturation density of N_s at 6 Å, n_x drops because of coalescence processes (Figures 5 and 6) in the interval of equivalent thickness from 6 to 12 Å. The density of the aggregates n_x, obtained under identical deposition conditions and thickness intervals, is greater for particles formed on the KCl substrate with Pb colloids in comparison with the KBr substrate with Cu colloids, and the mean diameter $\bar{D}$ of the aggregates is smaller, while the degree of coverage of the surface Z with aggregates is approximately the same. In the interval of equivalent thickness from 4.5 to 6 Å, the degree of epitaxial ordering S_{100} increases from 25 to 41%, remaining practically constant up to the equivalent thickness of 12 Å. Compared with the KBr substrate with Cu colloids for particles made under these same conditions on a KCl substrate with Pb colloids, with the exception of a smaller degree of epitaxial ordering, we can observe the existence of an initial domain in which S_{100} increases with time for

equivalent thickness of particles t (Figure 4). It should be mentioned that, in the interval of equivalent thickness from 4.5 to 6 Å, an increase occurs in both S_{100} and n_x. Among the aggregates formed on the KCl substrate with Pb colloids, aggregates in orientation (~~100~~ 111) are also observed in a small number (Table 2 and Figure 6). Deposition made at a substrate temperature of 260°C at the same deposition rate R differs in all parameters (n_x, Z, $\bar{D}$, S_{100}) in comparison with deposition made at a substrate temperature of 290°C (Table 2 and Figure 4). Along with an increase in the equivalent thickness of particles from 6 to 12 Å, there is an increase in the specific density n_x from 25 to 35 $\cdot 10^{10}$ aggregates per cm^2, in the degree of epitaxial ordering S_{100} from 0 to 23%, in the degree of coverage Z from 5 to 11%, and in the mean diameter $\bar{D}$ from 52 to 62 Å. It should also be mentioned that, under the same deposition conditions, the parameters n_x and S_{100} of the Au aggregates formed on the KBr substrate with Cu colloids remain practically constant for particles made at substrate temperatures of 260 and 290°C. Aggregates in orientation (111) are missing from the deposition made at a substrate temperature of 260°C. The rate of attaining the specific maximum density N_s of the Au aggregates made at the substrate temperature of 290°C at a deposition rate of 0.1 Å $\cdot s^{-1}$ is very different from the rate of attaining the maximum density N_s for aggregates formed with a deposition rate of 0.3 Å $\cdot s^{-1}$ (Figure 4).

3.3 NaCl Substrate ($1.2 \cdot 10^{10}$ cm^{-2} Cu Colloids) and Other NaCl Substrates

The results obtained for Au deposition on a NaCl substrate with Cu and Ag colloids are presented in Table 3, and Figures 7, 8 and 9.

The specific density n_x of the Au aggregates formed at a substrate temperature of 290°C, at a deposition rate of 0.3 Å $\cdot s^{-1}$, increases in the interval of equivalent thickness from 4.5 to 6 Å. After reaching the maximum saturation density N_s at the equivalent thickness of 6Å, n_x drops because of

the coalescence processes (Figures 8 and 9) in the domain of equivalent thickness from 6 to 9 Å, and increases again because of secondary nucleation at the equivalent thickness of 12 Å. The value of the specific density of the aggregates n_x is comparable to that obtained under similar deposition conditions on a KCl substrate with Pb colloids in the domain of equivalent thickness from 4.5 to 9 Å, both in value and in the appearance of dependence in comparison to the equivalent thickness of the particles. However, the degree of epitaxial orientation S_{100} is greatly decreased (Figures 7, 8 and 9), while the increase in S_{100} in the interval of equivalent thickness from 4.5 to 12 Å, from 0% to 6%, is very slight. On the other hand the percentage of Au aggregates in orientation (111), S_{111} is quite large, compared to the percentage found for the depositions made under the same conditions on a KBr substrate with Cu colloids and on KCl with Pb substrates. In particles with an equivalent thickness of 12 Å, S_{111} is equal to 14% of the maximum value for Au aggregates with the same morphology, and more than double the S_{100} (Table 3). The degree of coverage of the surface Z with aggregates has values close to those obtained by deposition on a KCl substrate with Pb colloids for equivalent thicknesses of 4.5, 6.0 and 9.0 Å, but the equivalent thickness of 12 Å records a value of 44%, compared to 28% for the KCl substrate with Pb colloids (Figures 4 and 7). A reduction in the substrate temperature from 290 to 260°C, while maintaining the deposition rate of 0.3 Å $\cdot$ s^{-1}, determines a drop in the specific density n_x of the Au aggregates, in the degree of S_{100} and S_{111} orientation, in the degree of coverage Z and in a reduction of the diameter $\bar{D}$ (Table 3). The most pronounced differences are recorded in deposition with equivalent thickness of 12 Å. Thus, while the degree of coverage Z with aggregates for particles made at a substrate temperature of 290°C with an equivalent thickness of 12 Å is 44%, it is only 8% for

particles with the same equivalent thickness made at a substrate temperature of 260°C (Table 3 and Figure 7).

The increase in the formation period of aggregates at a substrate temperature of 290°C in producing condensation at a deposition rate of 0.1 $\mathring{A} \cdot s^{-1}$, compared to that at 0.3 $\mathring{A} \cdot s^{-1}$, determines an increase in their specific density n_x and their degree of S_{100} and S_{111} orientation (Table 3 and Figure 7).

The kinetics of formation and degree of orientation of the Au aggregates condensed on a NaCl substrate with a density of $5.2 \cdot 10^8$ Cu colloids per cm^2 and on a NaCl substrate with a density of $3.6 \cdot 10^{10}$ Ag colloids per cm^2, are similar (Table 3).

4. Discussion

As can be judged from a series of works [1, 9, 13, 17-22], with a total existence of several m^2 of Au deposited for evaporation on alkali halide substrates, there still is not a satisfactory theory for the epitaxis or to specify the specific factors which govern the processes of oriented growth in the case of formation of thin layers through a process of nucleation and growth.

In a previous work [23], using the formalism of the atomistic theory of nucleation [15, 18, 24-28] and experimental results obtained by Adam and Harsdorff [29,30] on the degree of oriented growth of thin layers of Au as a function of deposition conditions on alkali halide substrates, we have demonstrated the fact that epitaxial growth can only be achieved under conditions of incomplete condensation. In accepting the hypotheses of the atomistic theory of nucleation [15, 18, 24-28], the condition of incomplete condensation is achieved under conditions in which the process of re-evaporation of the donor atoms is dominant. The fact that realization of the degree of epitaxis different in the Au thin layers, as a function of the alkali halide

substrates on which they are formed, has not been able to be demonstrated by parameters characteristic of the atomistic theory of nucleation [23], demonstrates the inadequacy of the phenomenological hypotheses admitted in the theory, especially for the condition of incomplete condensation. It should be mentioned that, in order to achieve more satisfactory correspondence between the experimental data and the theoretical description of the kinetics of Au aggregate formation on alkali halide substrates under conditions of incomplete condensation, the atomistic theory of nucleation should have considered the existence of aggregate mobility [15, 18, 24, 31, 32]. However, as Robins [24] has mentioned, this agreement has only been produced by means of mathematical calculation, while the intrinsic nature of aggregate mobility and of the coalescence determining it have not yet been explained.

Acknowledging the mobility of the aggregates implies realization of their coalescence, not only by growing together in a process of capturing donor atoms which diffuse on the substrate, but also by shock in the process of their migration. The interpretation of Harsdorff's theory [13, 16, 33] by Metois, Masson and Kern [34, 35] from experimental results stipulates the possibility of formation of epitaxially oriented aggregates through the coalescence of aggregates migrating on the substrate. These opinions [13, 16, 19, 22, 33] and experimental data [34, 35] provide support to buttress consideration of the formation of epitaxial aggregate as a post-nucleation phenomenon [19, 36], and this implies renunciation of the theories based on critical epitaxial nuclei [25].

In presenting the results of our experiments in forming Au aggregates on KBr, KCl_2 and NaCl substrates with colloidal centers, we have aimed at demonstrating the existence of the two dependencies mentioned:

a. the dynamic nature of the degree of epitaxial ordering, and variations in S_{100} with deposition times;

b. dependence of the degree of epitaxial ordering S_{100}, with respect to the phenomena of coalescence.

Our experimental data demonstrate the influence of the deposition time on the grade of epitaxial ordering S_{100}. Thus, by reducing the deposition rate from 0.3 $\mathring{A} \cdot s^{-1}$ to 0.1 $\mathring{A} \cdot s^{-1}$, we have succeeded in increasing the degree of epitaxial orientation S_{100}, and the Au aggregates with equivalent identical thickness formed at a substrate temperature of 290°C on KBr, KCl and NaCl substrates with colloids (Tables 2 and 3, Figures 1, 4 and 7). When Au is deposited on KCl substrates with Pb colloids at a substrate temperature of 290°C and at a deposition rate of 0.3 $\mathring{A} \cdot s^{-1}$, there is a significant growth (30%) in the degree of epitaxial orientation S_{100}, along with an increase in the equivalent thickness of the particles. However, the predominant role in producing Au aggregates of epitaxial orientation, as this study verifies, is the nature of the alkali halide substrates and the deposition conditions [8, 19, 39, 30, 37, 38].

Our experimental results have demonstrated that no direct connection can be established between the presence of phenomena of coalescence, secondary nucleation and the degree of epitaxial orientation S_{100}. Thus, the appearance of coalescence phenomena and of secondary nucleation in Au aggregates with an equivalent thickness of 12 $\mathring{A}$ formed at a temperature of 290°C on a substrate of KBr with Cu colloids and a substrate of KCl with Pb colloids does not modify the value of the degree of epitaxial orientation (Table 2, Figures 1, 2, 4 and 5). On the other hand, for Au aggregates with an equivalent thickness of 12 $\mathring{A}$ formed at a temperature of 290°C on a NaCl substrate with Cu colloids, the presence of coalescence phenomena and secondary nucleation

determine the greater growth in the degree of S_{111} orientation compared to the degree of epitaxial orientation S_{100}.

The kinetics of formation of Au aggregates on alkali halide substrates with colloidal centers, namely: the time for reaching the maximum saturation density N_s, the rate of increase in the mean diameter $\bar{D}$ of the aggregates and the degree of coverage Z with aggregates, along with the increase in the equivalent thickness t of the particles, demonstrates dependence with respect to the intrinsic nature of the alkali halide substrate and the deposition conditions.

5. Conclusions

The phenomenology of the processes of nucleation, aggregate mobility, aggregate crystalization, the formation of continuous metallic layers on alkali halide substrates, is primarily dependent on the intrinsic nature of the substrates and, secondarily, on the deposition conditions. In characterizing the intrinsic nature of the alkali halide substrates, it is necessary to take into consideration both the parameters of the material in the atomistic theory of nucleation [23] and the structure of defects in the substrates [18, 22, 39, 40], along with possible interaction at the aggregate-substrate interface.

References

1. C. J. Rossow, J. A. Kotze and C. A.O. Henning, Thin Solid Films, **29**, 85 (1975).
2. V. Topa, S. Ioan, B. Velicescu et. Ghe. Mitroaica, Rev. Roum. Phys., **18**, 571 (1973).
3. A. J. Donohoe and J. L. Robins, J. Cryst. Growth, **17**, 70 (1972).
4. H. Schmeisser, Thin Solid Films, **22**, 83 (1974).
5. A. Chambers, D. G. Lord and M. Prutton, Thin Solid Films, **6**, R$_1$ (1970).
6. S. Iso, D. Watanabe, S. Ogawa, J. Phys. Soc. Japan, **17**, 1071 (1962).
7. J. W. Matthews and E.Grünbaum, Appl. Phys. Letters, **5**, 106 (1964); Phil. Mag., **11**, 1233 (1965).
8. J. W. Matthews, J. Vac. Sci. Technol., **3**, 133 (1966).
9. H. Sato and S. Shinozaki, Surface Science, **21**, 229 (1970).

10. K. Mihama and Y. Yasuda, J. Phys. Soc. Japan, **21**, 1166 (1966).
11. S. Ino, J. Phys. Soc. Japan, **21**, 346 (1966).
12. S. Ino, and S. Ogawa, J. Phys. Soc. Japan, **22**, 1365 (1967).
13. M. Hansdorff, Thin Solid Films, **32**, 103 (1976).
14. S. Ino, D. Watanabe and S. Ogawa, J. Phys. Soc. Japan, **19**, 881 (1964)
15. J. A. Venables, Phil. Mag., **27**, 697 (1973).
16. A. Peskeppel and M. Hansdorff, Thin Solid Films, **35**, 99 (1976).
17. O. S. Heavens, Thin Solid Films, **32**, 117 (1976)
18. M. J. Stowell, J. Cryst. Growth, **24/25**, 15 (1974)
19. I. Bacci and H. Poppa, Thin Solid Films, **12**, 167 (1972)
20. J. B. Roos and L. S. Yeomans, J. Cryst. Growth, **13/14**, 217 (1972)
21. L. Holland, Vacuum, **24**, 153 (1973)
22. G. J. Distefano, Thin Solid Films, **32**, 157 (1976).
23. M. I. Bibilov et N. Poresco Pogarov, St. cerc. fiz., **29**, 23 (1977).
24. J. L. Robins, Thin Films, **32**, 151 (1976)
25. D. Walton, J. Chem. Phys., **37**, 2182 (1962).
26. G. Zinsmeister, Vacuum, **16**, 529 (1966).
27. B. Lewis and D. S. Campbell, J. Vac. Sci. Technol, **4**, 207 (1967).
28. B. Lewis, Surface Science, **21**, 273 (1970).
29. R. W. Adam, Z. Naturforsch. **23 a**, 1526 (1968).
30. M. Hansdorff, R. W. Adam and H. Schmeisser, Krist. Techn., **5**, 279 (1970).
31. M. J. Stowell, Thin Solid Films, **21**, 91 (1974).
32. J. L. Robins, Y. J. Dekoski and B. F. Usher, Jpn. J. Appl. Phys. Suppl., **2**, Part. 1, 1, 559 (1971).
33. M. Hansdorff, Z. Naturforsch. **23**, a, 1253 (1968).
34. J. F. Meiots, M. Gauch, A. Masson et R. Kern, Thin Solid Films, **11**, 205 (1972).
35. J. F. Meiots, J. C. Zanghi, R. Ehse et R. Kern, Thin Solid Films, **22**, 331 (1974).
36. D. W. Pashley, in *Epitaxial Growth*, Part. A, Edited by J. W. Matthews, Academic Press, 1975, p.2.
37. M. I. Bibilga, V. Topa and V. Teodorescu, Thin Solid Films, **32**, 209 (1976).
38. M. I. Bibilga, V. Topa, V. Teodorescu, Izv. Akad, Nauk, Ser Fiz., **41**, 2450 (1977).
39. M. José Yacaman and J. P. Hirth, Thin Solid Films, **38**, 215 (1976).
40. R. Uyeda, Thin Solid Films, **38**, 25 (1976).

Abstract

STUDY OF THE GROWTH OF VACUUM CONDENSED Au PARTICLES ONTO THE (100) SURFACES OF KBr KCl AND NaCl SUBSTRATES WITH COLLOIDAL CENTRES. 1. Introduction 2. Experimental methods and calculation of data. 3. Experimental results 4. Discussion. 5. Conclusions.
The present work refers to the experimental study by electronmicroscope and electrondiffraction of the formation kinetics and the orientation degree of the Au particles obtained by condensation in vacuum onto KBr, KCl and NaCl substrates with colloidal centres. The electronmicroscope images concerning the Au deposits of various equivalent thickness obtained onto the three alkali halides substrates, at various substrate temperatures and deposition rates were used in order to determine the following parameters: the particles specific density n_r, the ratios S_{100} and S_{111} of oriented particles, the degree Z of the surface coverage by the particles and the mean diameter $\bar{D}$ of the particles distribution. The obtained results are discussed in relation to the opinions of various workers on the phenomenology of the processes leading to the formation of oriented particles.

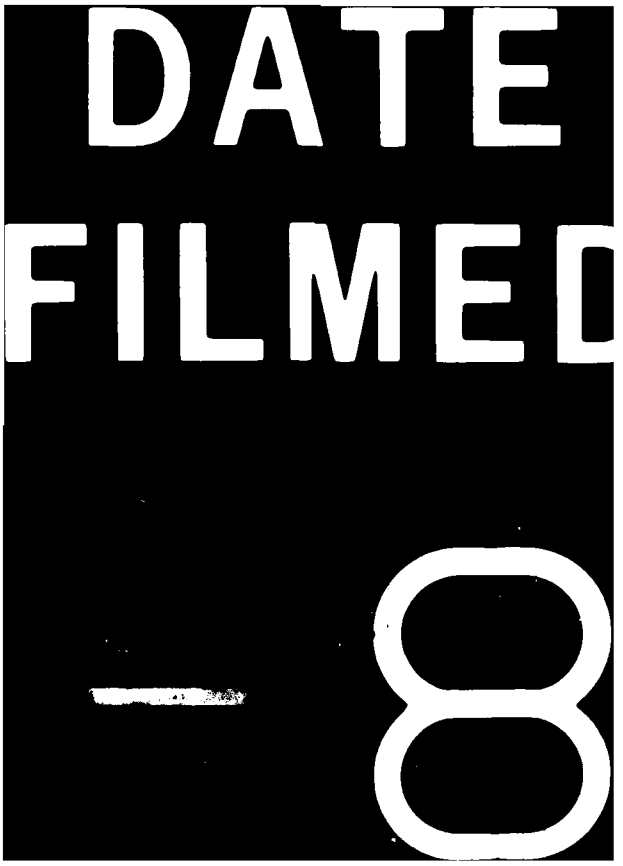
DATE
FILMED
8